Magnetic field dependence of high-T_{c} interface superconductivity in La_{1.55}Sr_{0.45}CuO_{4}/La_{2}CuO_{4} heterostructures

V. A. Gasparov, L. Drigo, A. Audouard, Xi He, and I. Božović

Phys. Rev. B **94**, 014507 — Published 11 July 2016

DOI: 10.1103/PhysRevB.94.014507

Magnetic field dependence of high-T_c interface superconductivity in $La_{1.55}Sr_{0.45}CuO_4/La_2CuO_4$ heterostructures

V. A. Gasparov[1], L. Drigo[2], A. Audouard[2], Xi He[3] and I. Božović[3,4]

[1]*Institute of Solid State Physics RAS, Chernogolovka, 142432, Russian Federation*
[2]*Laboratoire National des Champs Magnétiques Intenses (UPR 3228 CNRS, INSA, UGA, UPS), Toulouse, France*
[3]*Applied Physics Department, Yale University, New Haven CT 06520, USA*
[4]*Brookhaven National Laboratory, Upton, NY 11973, USA*

Abstract

Heterostructures made of a layer of a cuprate insulator, La_2CuO_4, on the top of a layer of a non-superconducting cuprate metal, $La_{1.55}Sr_{0.45}CuO_4$, show high-T_c interface superconductivity confined within a single CuO_2 plane. Given this extreme quasi-two-dimensional quantum confinement, it is of interest to find out how does interface superconductivity behave when exposed to an external magnetic field. With this motivation, we have performed contactless tunnel diode oscillator-based measurements in pulsed magnetic fields up to 56 T as well as measurements of the complex mutual inductance between a spiral coil and the film in static fields up to 3 T. Remarkably, we observe that interface superconductivity survives up to very high perpendicular fields, in excess of 40 T. In addition, the critical magnetic field $H_m(T)$ reveals an upward divergence with decreasing temperature, in line with vortex melting as in bulk superconducting cuprates.

I. INTRODUCTION

A. Critical behavior in two-dimensional superconductors

Superconductivity in conventional superconductors has been well accounted for by the Bardeen-Cooper-Schrieffer theory[1]. In these materials, the superconducting transition is typically rather sharp, and the critical fluctuation region very narrow, less than 1 mK wide. Hence, the critical temperature, T_c, and the critical fields, H_{c1} and (in type-2 superconductors) H_{c2}, are all sharply defined, and can be unambiguously read from e.g., the raw experimental magneto-transport data.

However, cuprates that show high-T_c superconductivity are quasi-two-dimensional. This is true, in particular, for $La_{2-x}Sr_xCuO_4$, the simplest of hole-doped cuprates, which we study here. For optimal doping ($x = 0.16$), the in-plane (screened) plasma frequency in this material is[2] about 0.8 eV, while the c-axis (Josephson) plasma frequency is[3] about 5 meV, i.e., ~160 times lower; in anisotropic three-dimensional model this would imply the c-axis effective mass about 2.5×10^4 higher than the in-plane effective mass $m^* \approx 4\ m_e$. This is clearly unphysical, showing that the three-dimensional model is inapplicable, and implying that that the individual $La_{2-x}Sr_xCuO_4$ layers are only weakly (Josephson) coupled[4-6]. This was shown most directly by biasing a bulk single crystal of $La_{2-x}Sr_xCuO_4$ with a dc voltage V and observing microwave emission at the frequency ν that satisfies the Josephson relation $\nu = (2e/h)V$, where h is the Planck constant and e the electron charge. This clearly shows that $La_{2-x}Sr_xCuO_4$ behaves like a native stack of intrinsic Josephson junctions.

In addition, $La_{2-x}Sr_xCuO_4$ and other cuprates are characterized by very low superfluid stiffness. Together with reduced effective dimensionality, this leads to a large increase in thermal fluctuations[8]. In consequence, one observes[1,9] broadened resistive transitions, thermally assisted flux flow, giant and quantum creep, vortex liquid and glassy states, etc. This makes the experimental determination of T_c ambiguous, since instead of a sharp critical temperature here we have a critical range that can be 10-20 K wide. Hence, in the literature one can find notions such as T_c^{onset}, $T_c^{offset} \equiv T_c(R=0)$, $T_c^{midpoint}$, etc., referring to different points at the $R(T)$ curve in the broad transition region. Moreover, there is a dependence on the frequency of the probe, since higher-frequency (radio-frequency to microwave to terahertz to optical) probes pick up superconducting fluctuations at progressively shorter time scales and higher temperatures[10-14].

The experimental determination of H_{c2} is subject to the same ambiguity, since a substantial portion of the phase diagram well above the $H_{c1}(T)$ line is occupied by a vortex-liquid phase[15]. In practice, H_{c2} is most frequently determined by using as the defining criterion the field at which the resistivity reaches say 50% or 90% of its 'normal state value' near the T_c onset. The drawbacks of this practice is not just that these criterions are arbitrary and the 100% point ill-defined, but more important, they all produce concave $H_{c2}(T)$ curves quite unlike the mean-field behavior of $H_{c2}(T)$ predicted by the standard Bardeen-Cooper-Schrieffer theory. The physical reason is that even a 99% criterion underestimates the mean-field $H_{c2}(T)$; the observed finite resistivity does not imply that all the Cooper pairs have been broken by the magnetic field but rather that vortices are flowing and causing dissipation[1,9,15,16]. For this reasons, in what follows, we denote by H_m the characteristic magnetic field at which the vortex lattice melts into a vortex liquid. While this field H_m is also subject to some uncertainty, we make sure that this does not affect our conclusions. H_m provides a conservative lower limit on the mean-field H_{c2}.

B. High-T_c interface superconductivity

High-T_c interface superconductivity in $La_{2-x}Sr_xCuO_4$-based heterostructures was first reported[17] back in 2002. Subsequent important advances include observation of high-T_c interface superconductivity in structures in which neither constituent material was superconducting *per se*. For example, heterostructures consisting of a layer of heavily overdoped $La_{1.55}Sr_{0.45}CuO_4$, which is metallic but not superconducting, and a layer of La_2CuO_4, which in itself is insulating, show high-T_c interface superconductivity[18] with $T_c \approx$ 30-35 K.

In the last decade or so, a large number of papers have been published that are related to high-T_c interface superconductivity in $La_{2-x}Sr_xCuO_4$-based heterostructures. Altogether, they present the results from a massive accumulated database, with well over a thousand $La_{2-x}Sr_xCuO_4$ bilayer samples studied by many techniques. All of these data, without exceptions, are consistent with high-T_c superconductivity being confined to a single CuO_2 plane, which furthermore can be identified (and to some extent controlled). Strong evidence comes from e.g., *c*-axis transport in heterostructures with one-unit-cell thick $La_{2-x}Sr_xCuO_4$ layers[19], the dependence of T_c on the thickness of $La_{1.55}Sr_{0.45}CuO_4$ and La_2CuO_4 layers[18], the critical current measurements in bilayer $La_{1.55}Sr_{0.45}CuO_4/La_2CuO_4$ heterostructures[18], and doping independence of T_c in bilayers[20]. One should also mention the perfect 2D scaling near the superconductor-insulator transition[21] in $La_{2-x}Sr_xCuO_4$. However, the most direct proof was achieved by a new technique, δ-doping tomography, specially invented for this purpose[22]. It relies on the known fact that doping $La_{2-x}Sr_xCuO_4$ with a small concentration of Zn atoms (which substitute for Cu) causes a dramatic reduction of T_c and the superfluid density. In $La_{2-x}Sr_xCuO_4$-based heterostructures, such a reduction is only observed when Zn dopant atoms are inserted in the second CuO_2 plane above

the nominal $La_{1.55}Sr_{0.45}CuO_4/La_2CuO_4$ interface. This demonstrated that high-T_c interface superconductivity is confined to a single CuO_2 plane in these heterostructures[22].

A separate question is whether the observed high-Tc interface superconductivity originates from a purely electronic mechanism (electron transfer across the interface, resulting in electron accumulation on one side and depletion on the other side of the interface), or from a chemical mechanism, i.e., cation intermixing between the two cuprate layers. In principle, one can generate quasi- two-dimensional high-T_c interface superconductivity confined to a single LSCO layer by either of these two methods — by near-optimal δ-doping with Sr in that particular layer, or by doping via charge transfer from a neighbour layer(s). Which of these two mechanisms dominates in a given sample can be differentiated by resonant X-ray scattering that can measure the profile of the density of mobile charge carriers within a film and can distinguish them from the cation density profile[23]. Applying this technique to LSCO-LCO heterostructures analogous to the one studied here, it has been shown that the first mechanism — electron redistribution across the interface— is dominant in this situation[23]. Independent evidence pointing to the same conclusion was obtained by reflection high-energy electron diffraction, time-of-flight ion scattering and recoil spectroscopy, scanning transmission electron microscopy, and high-resolution electron-energy loss spectroscopy[18], as well as by the coherent-Bragg-rod analysis, a synchrotron-based phase-retrieval X-ray diffraction technique[24]. The later has shown directly that Sr inter-diffusion is limited to a single LSCO layer, and is in fact asymmetric (Sr moves towards the substrate, due to epitaxial strain)[24].

It is an interesting question whether and how are the structures of individual vortices and of the vortex lattice, under the conditions of such extreme two-dimensional quantum confinement, modified compared to those in bulk samples. However, till now the *H-T* phase diagram of these ultrathin $La_{1.55}Sr_{0.45}CuO_4/La_2CuO_4$ heterostructures was explored neither theoretically nor experimentally.

II. EXPERIMENTAL RESULTS

Here we present the first *H-T* phase diagram of a high-quality ultrathin $La_{1.55}Sr_{0.45}CuO_4/La_2CuO_4$ heterostructure determined using the technique based on a radio-frequency tunnel diode oscillator. In zero field, the film shows high-T_c interface superconductivity with T_c = 31 K. As reported here, interface superconductivity survives up to very high magnetic fields $H_m(T)$, exceeding 40 T at the lowest temperature available in this experiment (T = 1.4 K).

The studied bilayer heterostructure consists of a five-unit-cells thick layer of a cuprate insulator, La_2CuO_4, on top of an equally thick layer of a non-superconducting cuprate metal, $La_{1.55}Sr_{0.45}CuO_4$. It was synthesized using an advanced atomic-layer-by-layer molecular beam epitaxy system that incorporates *in situ* surface science tools such as time-of-flight ion scattering and recoil spectroscopy and reflection high-energy electron diffraction. The film was grown on a $10\times10\times1$ mm^3 single-crystal $LaSrAlO_4$ substrate polished nearly perpendicular to the [001] crystallographic direction. The growth mechanism, microstructure and superconducting properties of similar $La_{1.55}Sr_{0.45}CuO_4/La_2CuO_4$ heterostructures synthesized by this technique have been reported previously[17-22]. Atomic-layer-by-layer molecular beam epitaxy technique enables synthesis of atomically smooth films as well as multilayers with sharp interfaces.

To determine H_m, we used radio-frequency measurements based on tunnel-diode oscillator device[25]. Given the thin film geometry, a pair of compensated single-layer flat spiral coils was used in pulsed-field experiments in order to compensate the voltages induced during a field pulse. One of these coils was positioned very close to the film surface (~ 0.2 mm), while the other was at a relatively large distance (2 mm) below the sample surface. These coils, together with a capacitor in parallel, constitute the inductive element of a resonant *LC* circuit powered by a tunnel-diode oscillator biased in the negative resistance region of the current-voltage characteristic. After signal amplification, mixing with a reference signal and demodulation, the resulting oscillator frequency, which can be approximated by $f = 1/(2\pi\sqrt{LC})$, lies in the MHz range. As the magnetic field increases, the tunnel-diode oscillator tracks the shift in the resonant frequency that increases upon entering the normal state, giving a clear indication of the superconducting-to-resistive state transition[26,27].

Measurements in pulsed magnetic fields were performed in the temperature range from 1.4 K to 35 K. The film was oriented with *H* either parallel or perpendicular to the CuO_2 planes. Similar radio-frequency measurements were performed on the same $La_{1.55}Sr_{0.45}CuO_4/La_2CuO_4$ heterostructure in static magnetic fields with *H*//c in the field range below 3 T. (The crystallographic *c*-axis is perpendicular to the CuO_2 planes.) In this radio-frequency technique, we measure the complex mutual inductance, *M*, between a film and a flat spiral coil located in the proximity of the film. The *LC* resonance circuit is driven by an impedance meter operating at 2-30 MHz, with a high frequency stability of 10 Hz. The film is placed in vacuum at about 0.2 mm above the coil; this allows the sample temperature to vary from 2 K to 50 K, while keeping the *LC* circuit at a constant temperature of 4.2 K. Changes in $M(H,T)$ are detected as changes of the resonance frequency, $f(H,T)$, and of the impedance, $Z(H,T)$, measured by an impedance meter tuned to the impedance resonance at different frequencies[28,29].

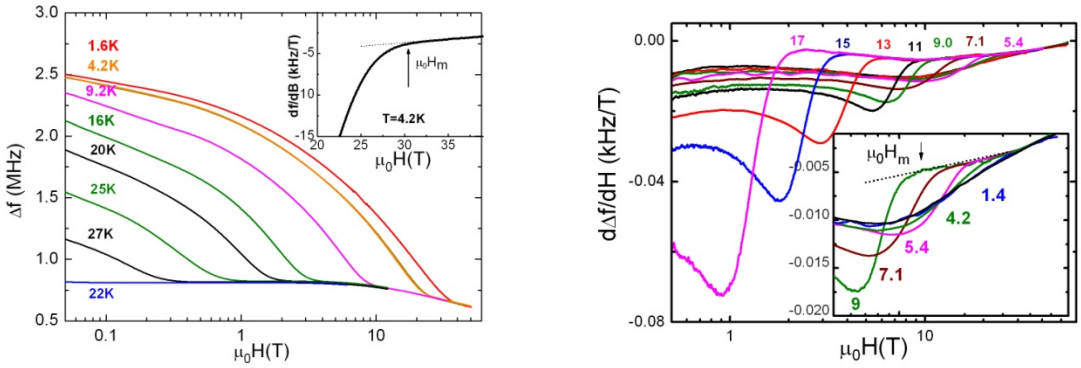

Figure 1 (Color online) (a) Field-dependent frequency changes in pulsed fields for *H*//*c*. The inset displays construction lines for the determination of the characteristic field H_m. (b) The first derivative of the frequency shift can be used to identify H_m more precisely. Temperatures are shown in Kelvin.

Figure 1 displays an example of field-dependent the derivative, $d(\Delta f)/dH$ in pulsed magnetic fields for temperatures in the range from 30.6 K down to 1.4 K. What remains in Fig. 1 is a feature observed in the entire explored temperature range. The point of deviation from the background curve yields a characteristic field, $H_m(T)$.

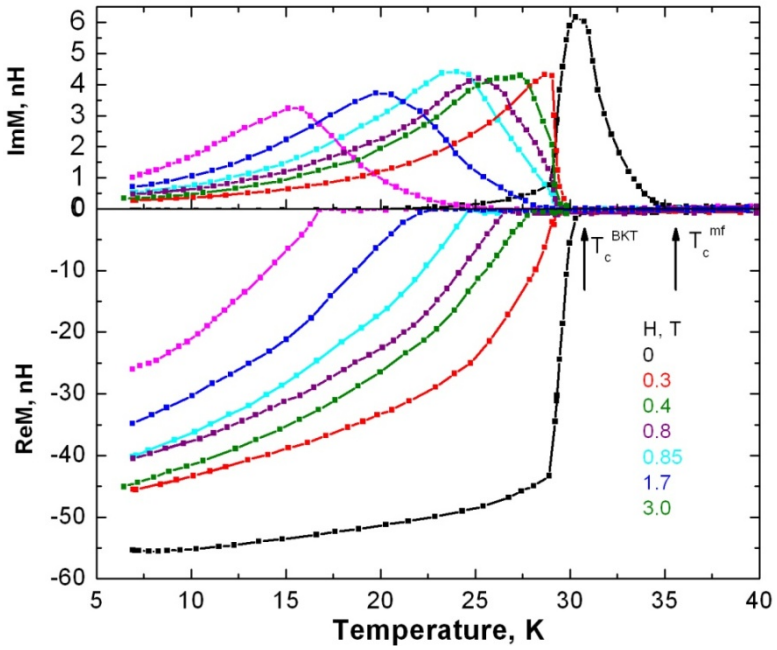

Figure 2. (Color online) *ReM(T)* and *ImM(T)* for magnetic field values in the range 0-2.9 T. T_c^{mf} and T_c^{BKT} are the Bardeen-Cooper-Schrieffer and Berezinskii-Kosterlitz-Thouless transition temperatures, respectively.

In Fig. 2 we show the temperature dependence of *ReM* and *ImM* measured at different magnetic fields. Note that the temperature at which *ReM*(*T*) starts to drop is lower than the temperature at which *ImM*(*T*) starts rising, by about ΔT_c = 5 K in zero field. Moreover, the sharp drop in Re*M*(*T*) indicates an equally sharp drop in the superfluid density at the same temperature. This observation is ascribed to the dynamic Berezinskii-Kosterlitz-Thouless transition[28,29]. Within this framework, the dynamic Berezinskii-Kosterlitz-Thouless transition at a given frequency occurs at the temperature $T^{\omega}_{\mathrm{BKT}}$ at which *ImM*(*T*) is the largest, and the correlation length $\xi^{+}(T)$ (i.e., the average distance between thermally induced free vortices and antivortices) becomes equal to the vortex diffusion length $l_\omega = (14D/\omega)^{1/2}$, where *D* is the vortex diffusion constant. In Fig. 2, we see that the dynamic Berezinskii-Kosterlitz-Thouless transition is completely removed by a very small magnetic field, $B \approx 0.3$ T. The field strength that destroys the vortex pairs, H_{dest}, can be estimated from the relation $l_\omega \sim a_v$, where $a_v = (\Phi_0/H_{dest})^{1/2}$ is the Abrikosov vortex lattice parameter, i.e., the scale limiting the formation of vortex–antivortex pairs in a magnetic field. From $l_\omega \sim a_v$, we estimate that a_v = 102 nm at H_{dest}, yielding H_{dest} = 0.2 T, close to what we observe.

At larger fields above H_{dest}, the dynamic Berezinskii-Kosterlitz-Thouless transition is absent as the antivortices are largely flipped out and only parallel vortices remain, and Re*M*(*T*) decreases gradually, without an apparent rapid drop. Nevertheless, the onsets in and Re*M*(*T*) and *ImM*(*T*) remain displaced, because *ImM*(*T*) starts to rise exponentially as soon as superconducting fluctuations become significant enough to cause a visible increase in the film conductivity, while *ReM*(*T*) onsets only when the global coherence is established, enabling the formation of supercurrent loops that are needed to screen the external magnetic field. The width of this

fluctuation range depends on how short is the time scale on which the superconductive fluctuations can be detected; it increases with the frequency of the measurement, to about 10 K in microwave[10,11] and over 20 K in terahertz[12-14] experiments.

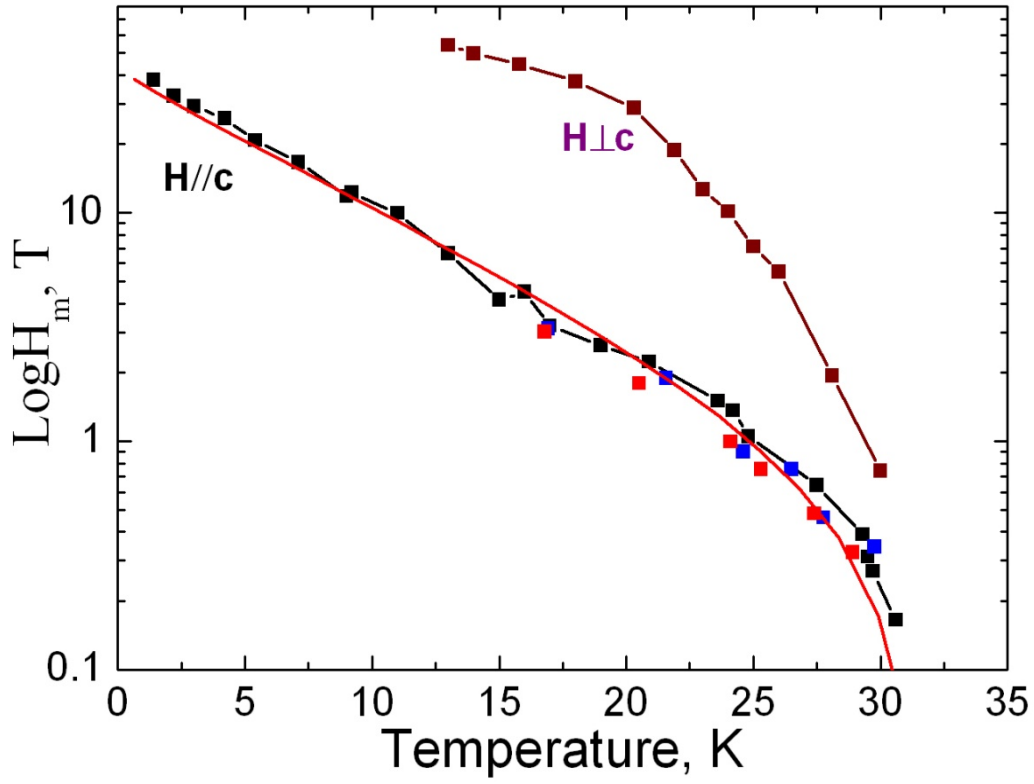

Figure 3. (Color online). Temperature dependence of H_m. Black squares indicate the values inferred from pulsed magnetic field experiments with *H//c* (see Fig. 1). Brown squares correspond to the data for *H⊥c*. Red and blue squares are the values of H_m inferred from the onset of *ReM(T)* and the maximum of *ImM(T)*, respectively, measured in static magnetic fields with *H//c*.

In Fig. 3, we show the temperature dependence of H_m, determined in few different ways. The black and brown squares indicate the values of H_m inferred from pulsed field experiments for *H//c* and *H⊥c*, respectively, while the red squares correspond to the onset of drop in *ReM*(*T*) and the blue squares correspond to the maximum of *ImM(T)* curves in Fig. 2. As observed, different criteria turn out very similar $H_m(T)$ dependences.

The kink field H_m can be regarded as the field at which vortices start flowing due to thermally activated melting[8,9,15,16]. It may be much smaller than H_{c2}, the field needed to break all Cooper pairs. At this point, much of the sample is still superconductive but phase slips disrupt the global phase coherence, so that the London penetration depth diverges. Within this framework, the melting transition field is given by[9]:

$$\frac{\sqrt{b_m(t)}}{1-b_m(t)}\frac{t}{\sqrt{1-t}}\left[\frac{4(\sqrt{2}-1)}{\sqrt{1-b_m(t)}}+1\right]=\frac{2\pi C_L^2}{\sqrt{Gi}} \quad (1)$$

Here $b_m = H_m/H_{c2}$ is the reduced melting field, $t = T/T_c$ is the reduced temperature, C_L is the Lindeman number and Gi is the Ginzburg number given by:

$$Gi = 0.5\left(\frac{k_B T_c \gamma}{H_c^2(0)\xi_0^3}\right)^2 \quad (2)$$

where $\gamma = \lambda_c/\lambda_{ab}$ is the anisotropy ratio (λ_{ab} and λ_c are the magnetic penetration depth parallel and perpendicular to *ab* plane). From our two-coil inductance measurements, we know that $\lambda_{ab}(0) \approx$ 230 nm, but for $La_{1.55}Sr_{0.45}CuO_4/La_2CuO_4$ heterostructures λ_c is unfortunately not known. Thus we treat the right-hand side of eq. (1) as a fitting parameter $A = 2\pi C_L^2/\sqrt{Gi}$. For $A = 0.7$ we get a very good fit in the whole explored temperature range, supporting the interpretation of $H_m(T)$ as the actual melting transition field.

In Fig. 3, one can also notice a downturn of $H_m(T)$ for $H \perp c$, i.e. parallel to the superconducting interface layer. For this field direction, the superconductor might enter a spatially-modulated Fulde, Ferrell, Larkin and Ovchinnikov state at low temperatures[30,31]. Actually, indications of this state have been observed in several 2D organic superconductors[32]. However, in order to drive the high-T_c superconducting layer to the normal state at low temperatures where Fulde-Ferrell-Larkin-Ovchinnikov effect could be observed, significantly larger magnetic fields may be necessary.

III. DISCUSSION AND CONCLUSIONS

While this is the first report of the *H-T* phase diagram of $La_{1.55}Sr_{0.45}CuO_4/La_2CuO_4$ heterostructures, there has been much previous study of quasi-two-dimensional superconductors, both theoretical and experimental, and many results apply to the present situation[33-60]. It is well known that quasi-two-dimensional systems are unstable to thermal fluctuations that destroy the true long-range order[33,34]. However, at low-temperature a quasi-ordered phase can form with a correlation function that shows a power-law decrease with the distance, in contrast to the exponential decay of correlations in the high-temperature disordered phase[35-38]. In such quasi-two-dimensional physical systems, vortex-antivortex pairs are thermally generated as low-energy excitations, but at low temperatures they are bound, do not move with the current, and hence cause no dissipation. Thus, superconductivity is possible[39,40] in such systems, including ultra-thin films, heterostructures and superlattices, as well as in naturally layered materials, as long as the layer sheet resistance is lower than the pair quantum resistance ($h/4e^2 = 6.45$ kΩ).[21,41,42]

As the temperature is increased, the pairs get broken, which triggers vortex flow and finite resistivity. In neutral superfluids, this occurs at a sharp Berezinskii-Kosterlitz–Thouless phase transition[35-37]. While there has been much confusion about this in the literature, such a transition does not occur in superconductors at *dc* and low frequencies, because of vortex screening[43-47]. However, a dynamic Berezinskii-Kosterlitz–Thouless phase transition is possible at high enough frequencies[48,49], and has in fact been observed in teraherz experiments with both Bi-based[12] and La-based[13] cuprates as well as in radio-frequency experiments on $La_{1.55}Sr_{0.45}CuO_4/La_2CuO_4$ heterostructures[28,29], as indeed confirmed in the present experiments.

Much further evidence has been reported of quasi-two-dimensional nature of superconductivity in $La_{2-x}Sr_xCuO_4$ as well as various other cuprates[50-52], including observation of free vortices[53,54] at temperatures well above T_c. One should mention analogous observations in various other layered superconducting materials and ultrathin films, both inorganic and organic[55-60], a detailed review of which is beyond the scope of the present paper.

In conclusion, measurements of the complex mutual inductance between a spiral coil and an ultrathin $La_{1.55}Sr_{0.45}CuO_4/La_2CuO_4$ heterostructure for *H//c* reveal similar temperature dependence of both the onset in *ReM*(*T*) and the maximum of *ImM*(*T*). In zero field, *ReM*(*T*) — and thus the superfluid density — shows a very sharp drop, a signature of the dynamic Berezinskii-Kosterlitz-Thouless transition, which disappears in magnetic fields above 0.2 T. The onset of *ImM*(*T*) occurs at higher temperature then in Re*M*(*T*), because superconducting fluctuations increase the conductivity even without achieving the global phase coherence, in agreement with previous microwave and terahertz observations in cuprates. The temperature dependence of the critical magnetic field $H_m(T)$ shows an upward divergence as the temperature decreases down to 1.4 K. This behavior, which is quantitatively accounted for by vortex melting transition at H_m, is similar to what is observed in bulk superconducting cuprates and some other quasi-two-dimensional superconductors. The main surprise here is that in ultrathin $La_{1.55}Sr_{0.45}CuO_4/La_2CuO_4$ heterostructures superconductivity is remarkably resilient to magnetic field, surviving in the field of 40 T.

Acknowledgments

We would like to thank A. Koshelev for valuable discussions. This work has been supported by the CNRS - Russian Academy of Sciences cooperation agreement n° EDC26086, the Russian Academy of Sciences Program "Quantum mesoscopic and non-homogeneous systems" and the Russian Foundation for Basic Research grant 12-02-00171. The support of the European Magnetic Field Laboratory (EMFL) is acknowledged as well. ALL-MBE synthesis and sample characterization were done at Brookhaven (I.B.) and supported by U.S. Department of Energy, Basic Energy Sciences, Materials Sciences and Engineering Division. X.H. is supported by the Gordon and Betty Moore Foundation's EPiQS Initiative through Grant GBMF4410.

References

1. M. Tinkham, in Introduction to Superconductivity, 2nd ed. (McGraw Hill, New York, 1996).
2. J. H. Kim, I. Bozovic, C. B. Eom, T. H. Geballe and J. S. Harris Jr., Physica C **174**, 435 (1991).
3. K. Tamasaku, Y. Nakamura and S. Uchida, Phys. Rev. Lett. **69**, 1455 (1992).

4. W. E. Lawrence and S. Doniach, in *Proceedings of the 12th International Conference on Low-Temperature Physics*, E. Kanda, ed. (Keigaku, Tokyo, 1971) p. 361.
5. L.N. Bulaevskii, JETP **37**, 1133 (1973).
6. R. A. Klemm, A. Luther, and M. R. Beasley, Phys. Rev. B **12**, 877 (1975).
7. Y. Kubo, A. O. Sboychakov, F. Nori, Y. Takahide, S. Ueda, I. Tanaka, A. T. M. N. Islam and Y. Takano, Phys. Rev. B **86**, 144532 (2012) and references therein.
8. V. J. Emery and S. A. Kivelson, Nature (London) **374**, 434 (1995).
9. G. Blatter, M. Y. Feigel'mann, Y. B. Geshkenbein, A. I. Larkin and V. M. Vinokur, Rev. Mod. Phys. **66**, 1125 (1994).
10. M. S. Grbić *et al.,* Phys. Rev. B **80**, 094511 (2009).
11. M. S. Grbić *et al.,* Phys. Rev. B **83**, 144508 (2011).
12. J. Corson *et al.,* Nature **398**, 221 (1999).
13. L. S. Bilbro *et al.*, Nature Phys. **7**, 298 (2011).
14. I. Madan *et al.*, Sci. Rept. **4**, 5656 (2014).
15. B. J. Ramshaw *et al.*, Phys. Rev. B **86**, 174501 (2012).
16. D. Majer, E. Zeldov and M. Konczykowskii, Phys. Rev. Lett. **75**, 1166 (1995).
17. I. Božović, G. Logvenov, I. Belca, B. Narimbetov and I. Sveklo, Phys. Rev. Lett. **89**, 107001 (2002).
18. A. Gozar *et al.*, Nature **455**, 782 (2008).
19. I. Bozovic, *et al.*, Nature (London) **422**, 873 (2003).
20. J. Wu *et al.*, Nature Materials **12**, 877 (2013).
21. A. T. Bollinger *et al.*, Nature **472** (London), 458 (2011).
22. G. Logvenov, A. Gozar and I. Božović, Science **326**, 699 (2009).
23. S. Smadici, *et al.*, Phys. Rev. Lett. **102**, 107004 (2009).
24. Y. Yacoby, H. Zhou, R. Pindak and I. Božović, Phys. Rev. B **87**, 014108 (2013).
25. L. Drigo, F. Durantel, A. Audouard and G. Ballon, Eur. Phys. J. Appl. Phys. **52**, 10401(2010).
26. A. Audouard *et al.*, Europhys. Lett. **109**, 27003 (2015).
27. V. A. Gasparov *et al.*, Phys. Rev. B **87**, 094508 (2013).
28. V. A. Gasparov and I. Božović, Phys. Rev. B **86**, 094523 (2012).
29. V. A. Gasparov *et al.,* Int. J. Mod. Phys. B **29**, 1542012 (2015).
30. P. Fulde and R. A. Ferrell, Phys. Rev. A **135,** 550 (1964).
31. A. I. Larkin and Yu. N. Ovchinnikov, Sov. Phys. JETP **20**, 762 (1965).
32. G. Zwicknagl and J. Wosnitza, Int. J. Mod. Phys. B **24**, 3915 (2010).
33. N. D. Mermin and H. Wagner, Phys. Rev. Lett. 17, 1133 (1966).
34. P. C. Hohenberg, Phys. Rev. **158**, 383 (1967).
35. V. L. Berezinskii, Sov. Phys. JETP **32**, 493 (1971).
36. V. L. Berezinskii, Sov. Phys. JETP **34**, 610 (1972).
37. J. M. Kosterlitz and D. J. Thouless, J. Phys. C 6, 1181 (1973).
38. B. I. Halperin and D. R. Nelson, J. Low Temp. Phys. **36**, 599 (1979).
39. V. L. Ginzburg, Phys. Scripta **27**, 76 (1989).
40. M. Randeria, J-M. Duan and L.-Y. Shieh, Phys. Rev. B **41**, 327 (1990).
41. D. B. Haviland, Y. Liu and A. M. Goldman, Phys. Rev. Lett. **62**, 2180 (1989).
42. X. Leng, J. Garcia-Barriocanal, S. Bose, Y. Lee and A. M. Goldman, Phys. Rev. Lett. **107**, 027001 (2011).
43. M. R. Beasley, J. E. Mooij and T. P. Orlando, Phys. Rev. Lett. **42**, 1165 (1979).

44. J. M. Repaci, C. Kwon, Q. Li, X. Jiang, T. Venkatessan, R. E. Glover, C. J. Lobb and R. S. Newrock, Phys. Rev. B **54**, 9674 (1996).
45. M. C. Sullivan, T. Frederiksen, J. M. Repaci, D. R. Strachan, R. A. Ott and C. J. Lobb, Phys. Rev. B **70**, 140503(R) (2004).
46. A. Gurevich and V. M. Vinokur, Phys. Rev. Lett. **100**, 227007 (2008).
47. V. G. Kogan, Phys. Rev. B **75**, 064514 (2007).
48. P. Minnhagen, Rev. Mod. Phys. **59**, 1001 (1987).
49. A. Jonsson and P. Minnhagen, Phys. Rev. B **55**, 9035 (1997)
50. C. Rogers, K. Luther-Myers, J. N. Eckstein and I. Bozovic, Phys. Rev. Lett. **69**, 160 (1992).
51. I. Bozovic, J. N. Eckstein, M. E. Klausmeier-Brown and G. F Virshup, J. Supercond. **5**, 19 (1992).
52. S. Maekawa and T. Tohyama, Rept. Prog. Phys. **64**, 383 (2001).
53. L. Li *et al.,* Phys. Rev. B **81**, 054510 (2010).
54. Z. A. Xu, N. P. Ong, Y. Wang, T. Kakeshita and S. Uchida, Nature (London) **406**, 486 (2000).
55. S. Uji *et al.,* Nature (London) **410**, 908 (2001).
56. J. Singleton and C. Mielke, Contemp. Phys. **43**, 63 (2002).
57. K. Takada *et al.,* Nature (London) **422**, 53 (2003).
58. J. W. Clark *et al.,* Phys. Repts. **391**, 123 (2004).
59. F. Kagawa, K. Miyagawa and K. Kanoda, Nature (London) **436**, 534 (2005).
60. T. Zhang *et al.,* Nature Physics **6**, 104 (2010).